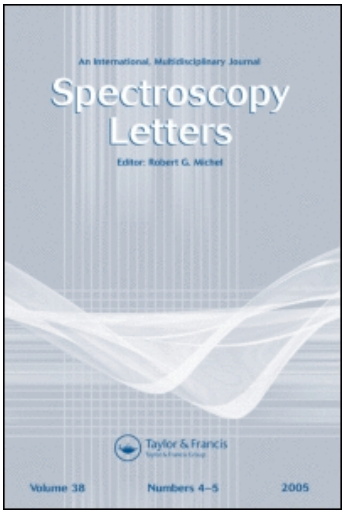

Spectroscopy Letters
Publication details, including instructions for authors and subscription information:
http://www.informaworld.com/smpp/title~content=t713597299

Raman Spectrum of Procaine Hydrochloride

M. Alcolea Palafox[a]
[a] Departamento de Química-Física I (Espectroscopia), Facultad de Ciencias Quimicas, Universidad Complutense, Madrid, SPAIN

To cite this Article Palafox, M. Alcolea(1997) 'Raman Spectrum of Procaine Hydrochloride', Spectroscopy Letters, 30: 6, 975 — 998
To link to this Article: DOI: 10.1080/00387019708006701
URL: http://dx.doi.org/10.1080/00387019708006701

SPECTROSCOPY LETTERS, 30(6), 975-998 (1997)

RAMAN SPECTRUM OF PROCAINE HYDROCHLORIDE

Key words: Vibrational frequencies, Raman spectrum, local anesthetics, procaine

M. Alcolea Palafox

Departamento de Química-Física I (Espectroscopia), Facultad de Ciencias Químicas, Universidad Complutense, 28040-Madrid, SPAIN

ABSTRACT

A vibrational study of the local anesthetic procaine hydrochloride in the solid state and in aqueous solution was carried out. Assignment of the amino groups was performed using deuterated and non-deuterated samples. All the bands in the spectra were identified and assigned. The structure of the procaine cation was determined using the AM1 semi-empirical method. A comparison with crystallographic data was made. The frequencies and intensities of the vibrations were also computed using AM1. Vibrational scale factors were employed in the AM1 calculations.

INTRODUCTION

Procaine and its derivatives[1,2] make up an important class of synthetic molecules in the therapeutic group of local anesthetics. Procaine (2-diethylaminoethyl *p*-aminobenzoate) is a local anesthetic remarkably similar in structure (Figure 1) to natural compounds actively participating in nerve impulse transmission. The conformation of the alkylamino end of the molecule, the quinonoidal character of the *p*-aminobenzoate group, and the proximity of the carbonyl oxygen to the ammonium nitrogen are considered necessary for effective interaction with receptors.

Although identification of the active form of the drugs has been controversial for some time, recent evidence seems to point to the cationic form as the active form, blocking the excitability from inside the nerve membrane.

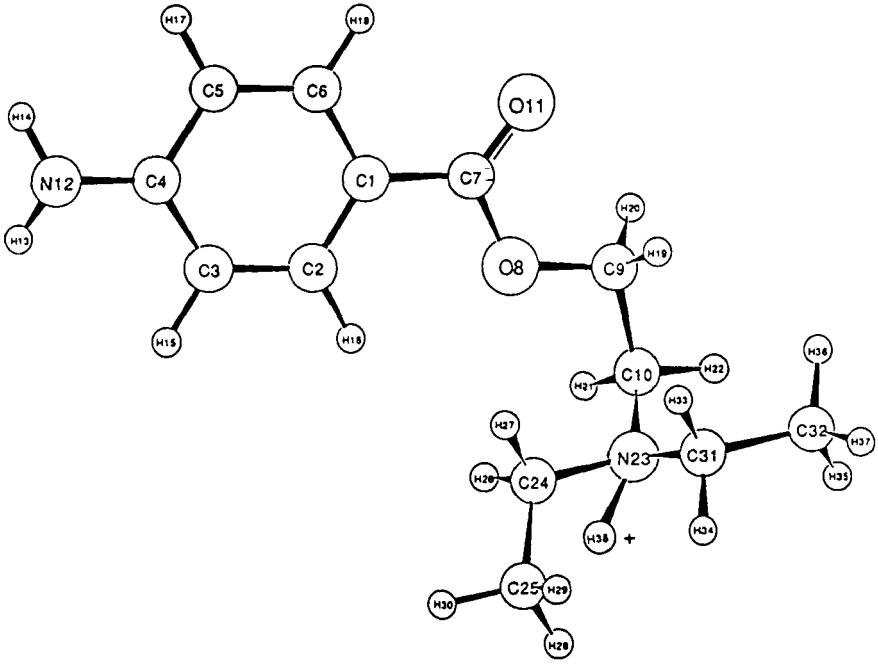

Fig. 1. Cation of procaine hydrochloride.

The notion that local anesthetics penetrate tissues as uncharged molecules and act at the membrane as cations provides an explanation for the fact that nearly all of the most effective local anesthetics are amines. Thus, in the present work it was considered important to carry out a comparative analysis of the geometrical results for different procaine cations with those computed by the AM1 semi-empirical method. A previous investigation had shown the suitability of AM1 and furnished a comparison with the MINDO/3 and MNDO methods[3].

As first step in the study of the anaesthesia, the infrared and Raman spectra of several local anesthetics were recorded and thoroughly interpreted[3-5]. In the present paper, the Raman spectra of procaine hydrochloride (PRC-HCL) in the solid state and in aqueous solution were undertaken, since this might shed light on the structure and activity relationship of other local anesthetics. Laser Raman spectroscopy permits the study of samples in aqueous solution,

in which biological processes like the phenomenon of anesthesia mainly take place.

EXPERIMENTAL

Samples of procaine hydrochloride from Merck were used without further purification (99 %). D_2O was from the Spanish Junta de Energia Nuclear (Nuclear Energy Commission), and had a purity of 99.7 %. For recording the spectra in the solid state, samples were inserted in a glass capillary as crystalline powder. For the aqueous solutions, PRC-HCL was dissolved to 40 % in weight, close to saturation. The spectra were recorded in special glass U-cells.

Deuterated samples were prepared by several procedures[5]. In the solid state the simplest one was: In a glass tube, PRC-HCL was solved with agitation in an excess of D_2O. The sample was gently warmed for 20 min. and afterwards dried in a vacuum oven. The procedure was repeated successively until the desired degree of deuteration for determination of spectra bands was obtained.

In aqueous solution, the deuteration of PRC-HCL was carried out mainly by adding D_2O to the desired concentration and then shaking for 15 minutes.

Raman spectra in the range 100-4000 cm^{-1} were recorded on a Laser-Raman JOBIN-YVON spectrophotometer RAMANOR U-1000 model, which has a double monochromator with halographic net planes and photon-counter detector. The Laser was a model 165, 2 ω ionized argon laser from SPECTRA PHYSICS. The laser power used was 100-400 mW and the slit widths were 100-400 μm.

COMPUTATIONAL METHODS

The calculations for procaine hydrochloride, represented by the PRC-H^+ cation, were carried out by using the standard AM1 procedure, as implemented in the AMPAC package of computer programs, which has provided accurate computational tools for analyzing problems relating to molecular structure and reaction mechanisms[6-8]. The geometry was determined by minimizing the energy with respect to all geometrical parameters without imposing molecular symmetry constraints. The PRC-H^+ cation was theoretically considered and analyzed as a molecule of procaine with a proton on the N(23) atom, the charge on the system being +1. The GAUSSIAN 90 and 92 packages[9] were also used. All the calculations were performed accordingly.

The DRAW program[10] was used to evaluate graphically the correctness of the geometries and plot the motions for each vibration, in our case 108 for PRC-HCL, thus providing identification and assignment of all the vibrations calculated theoretically. The graphic representations were observed on Tektronic model-4105 high-resolution computer terminals.

The Figures obtained were prepared on a Macintosh microcomputer using the BALL and STICK program[11].

RESULTS AND DISCUSSION

GEOMETRY OPTIMIZATION

The data on bond lengths, bond angles, and torsional angles for the procaine cation (PRC-H^+), obtained by the AM1 method are listed in Tables 1-3

Table 1. Optimized bond lengths in Å for the PRC-H$^+$ cation computed by the AM1 method and experimental values reported for several salts.

Bond length	Calculated	X-ray				
	AM1	PRC-HCL[a]	PRC-HICL[b]	PRC-NDG[c]	PRC-DPH[d]	PRC-PNP[e]
C(1)-C(2)	1.4029	1.36	1.396(4)	1.399(6)	1.386(4)	1.410(7)
C(2)-C(3)	1.3820	1.37	1.367(4)	1.387(5)	1.370(4)	1.369(7)
C(3)-C(4)	1.4252	1.41	1.405(4)	1.405(5)	1.400(3)	1.404(6)
C(4)-C(5)	1.4253	1.36	1.407(5)	1.399(6)	1.395(4)	1.390(8)
C(1)-C(6)	1.4070	1.41	1.409(4)	1.389(6)	1.394(2)	1.393(6)
C(5)-C(6)	1.3809	1.36	1.356(5)	1.400(5)	1.364(3)	1.381(8)
C(1)-C(7)	1.4509	1.47	1.457(4)	1.477(5)	1.461(3)	1.461(6)
C(7)-O(8)	1.3951	1.36	1.356(4)	1.364(5)	1.346(2)	1.364(4)
O(8)-C(9)	1.4262	1.44	1.427(4)	1.437(5)	1.440(2)	1.447(5)
C(9)-C(10)	1.5333	1.50	1.503(5)	1.514(7)	1.499(3)	1.505(6)
C(7)=O(11)	1.2332	1.22	1.210(4)	1.202(6)	1.206(3)	1.212(5)
C(4)-N(12)	1.3658	1.40	1.359(4)	1.385(4)	1.357(3)	1.377(7)
N(12)-H(13)	0.9880		0.72(4)			0.83(5)
N(12)-H(14)	0.9882		0.81(3)			0.85(3)
C(9)-H(19)	1.1223		0.91(3)			
C(9)-H(20)	1.1220		0.85(3)			
C(10)-N(23)	1.4949	1.51	1.505(4)	1.503(6)	1.505(2)	1.492(6)
N(23)-C(24)	1.5032	1.52	1.506(4)	1.513(6)	1.498(3)	1.515(5)
C(24)-C(25)	1.5141	1.49	1.508(5)	1.506(8)	1.493(3)	1.49(1)
N(23)-C(31)	1.5019	1.48	1.512(4)	1.508(6)	1.509(2)	1.492(7)
C(31)-C(32)	1.5138	1.49	1.511(6)	1.503(8)	1.508(3)	1.522(8)
N(23)-H$^+$(38)	1.0304		0.87(3)			1.00(4)

[a]From ref. 12. [b]From ref. 13. [c]From ref. 16. [d]From ref. 14. [e]From ref. 15.

respectively, with the corresponding experimental values reported for five procaine salts.

Bond lengths and angles within the PRC cation do not differ significantly in the crystal structures from those computed by AM1. The values for the hydrochloride salt[12] (PRC-HCL), which are in general very different from those calculated in a later study of the hydrochloride molecule[13] and from other experimental data[14-16], constitute an exception. The C-N bonds in the trialkylammonium group are in very good agreement with those observed in the crystal: the mean value of 1.50 Å exceeds the C-N single bond length by about 0.03 Å, which is probably associated with the larger coordination number of the protonated nitrogen atom. The environment about the N(23) atom is essentially tetrahedral, and the CNC angles in this group average

Table 2. Optimized bond angles in degrees for the PRC-H^+ cation computed by the AM1 method and experimental values reported for several salts.

Bond angle	Calculated	X-ray				
	AM1	PRC-HCL[a]	PRC-HCL[b]	PRC-NDG[c]	PRC-DPH[d]	PRC-PNP[e]
C(1)-C(2)-C(3)	120.8	122	121.9(3)	120.3(4)	121.1(2)	120.5(4)
C(2)-C(3)-C(4)	120.5	120	121.1(3)	120.2(4)	121.1(2)	121.1(5)
C(3)-C(4)-C(5)	118.2	118	116.9(3)	119.8(3)	117.7(2)	118.5(5)
C(1)-C(6)-C(5)	120.7	120	121.7(3)	121.1(4)	121.6(2)	121.1(5)
C(2)-C(1)-C(6)	119.3	118	116.8(3)	119.4(4)	117.8(2)	118.3(4)
C(4)-C(5)-C(6)	120.5	122	121.5(3)	119.2(3)	120.7(2)	120.6(4)
C(2)-C(1)-C(7)	122.4	124	123.7(3)	121.6(4)	123.0(2)	123.1(3)
C(6)-C(1)-C(7)	118.3	118	119.5(3)	119.0(4)	119.2(2)	118.7(4)
C(1)-C(7)-O(8)	114.3	112	112.9(3)	111.4(3)	112.7(2)	114.5(3)
C(7)-O(8)-C(9)	115.3	116		115.7(3)	116.5(2)	114.0(3)
O-C(9)-C(10)	103.9	109	104.7(3)	107.8(4)	108.6(2)	110.0(4)
C(1)-C(7)=O	130.5	128	126.2(3)	126.0(4)	125.6(2)	124.6(3)
O(8)-C(7)=O	115.1	120	121.0(3)	122.6(4)	121.7(2)	120.9(4)
C(3)-C(4)-N	120.9	119	121.2(3)	117.3(3)	120.8(2)	122.0(5)
C(5)-C(4)-N	120.9	123	121.8(3)	122.9(3)	121.5(2)	119.5(4)
C(4)-N-H(13)	120.3					123(3)
C(4)-N-H(14)	120.3					128(3)
H(13)-N-H(14)	119.3					109(4)
C(9)-C(10)-N	114.3	116	116.1(3)	113.4(4)	117.0(1)	113.5(4)
C(10)-N-C(24)	111.5	114	114.5(2)	113.1(3)	113.9(2)	110.5(4)
N-C(24)-C(25)	113.3	110	112.2(3)	114.6(4)	112.8(1)	117.1(5)
C(10)-N-C(31)	112.2	112	112.1(2)	110.9(3)	112.4(1)	113.7(3)
C(24)-N-C(31)	111.0	112	112.7(2)	113.2(3)	112.6(1)	112.6(4)
N-C(31)-C(32)	113.6	113	112.2(3)	111.8(4)	112.1(2)	113.4(5)
C(10)-N-H^+(38)	106.7					101(2)
C(24)-N-H^+(38)	107.7					108(2)
C(31)-N-H^+(38)	107.4					110(2)

[a]From ref. 12. [b]From ref. 13. [c]From ref. 16. [d]From ref. 14. [e]From ref. 15.

112.3°. The dimensions of the *p*-aminobenzoate group predicted by AM1 are in good agreement with those reported for *p*-aminobenzoic acid[17]. There were slight differences in the dimensions computed by AM1 for the *ester* and the free acid occur in the carboxylate group.

For the ring, AM1 predicts the same small but significant contribution of the quinonoid structure found in *p*-aminobenzoic acid and PRC salts. The average value of the central bond length in the benzene ring (1.381 Å) and the mean of the remaining ring C-C bond lengths (1.415 Å) are close to those in the

Table 3. Optimized torsional angles in degrees for PRC-H$^+$ cation computed by the AM1 method and reported experimentally in several salts.

Torsional Angles	Calculated	X-ray			Torsional Angles	Calculated
	AM1	PRC-HCL[a]	PRC-DPH[b]	PRC-PNP[c]		AM1
C(1)-C(2)-C(3)-C(4)	0.1				C(6)-C(5)-C(4)-N(12)	179.8
C(1)-C(6)-C(5)-C(4)	0.0				O-C(9)-C(10)-H(21)	-49.8
C(1)-C(7)-O(8)-C(9)	179.3	178.7	178.6	176.1	O-C(9)-C(10)-H(22)	68.3
C(2)-C(1)-C(6)-C(5)	0.0				C(10)-N-C(24)-H(26)	32.7
C(2)-C(1)-C(7)-O(8)	-0.4	6.6	5.9	2.9	C(10)-N-C(24)-H(27)	-83.8
C(2)-C(1)-C(7)=O	179.8	-173.7	-175.0	-178.2	C(10)-N-C(31)-H(33)	50.6
C(2)-C(3)-C(4)-N	-179.8				C(10)-N-C(31)-H(34)	167.0
C(3)-C(4)-C(5)-C(6)	0.1				H(20)-C-C(10)-H(21)	-167.8
C(3)-C(2)-C(1)-C(6)	0.0				H(20)-C-C(10)-H(22)	-49.7
C(3)-C(2)-C(1)-C(7)	180.0				H(19)-C(9)-C(10)-N	-52.4
C(3)-C(4)-N-H(13)	-1.4				H(20)-C(9)-C(10)-N	71.4
C(6)-C(1)-C(7)-O(8)	179.6	-172.7	-173.2	-177.0	N-C(24)-C(25)-H(28)	-59.5
C(6)-C(1)-C(7)=O	-0.2	7.0	6.0	1.9	N-C(24)-C(25)-H(29)	63.1
C(7)-O-C(9)-C(10)	179.0	173.3	-165.6	-178.8	N-C(24)-C(25)-H(30)	-178.1
C(7)-O-C(9)-H(19)	58.7				N-C(31)-C(32)-H(35)	-56.6
C(7)-O-C(9)-H(20)	-61.1				N-C(31)-C(32)-H(36)	66.1
O(8)-C(9)-C(10)-N	-170.7	70.1	-72.2	-65.1	N-C(31)-C(32)-H(37)	-175.3
C(9)-O-C(7)=O(11)	-0.8	1.0	-0.6	-2.8	C(25)-C(24)-N-C(31)	-80.2
C(9)-C(10)-N-C(24)	58.4	-61.4	-60.8	-150	C(25)-C(24)-N-H$^+$	37.0
C(9)-C(10)-N-C(31)	-66.8	69.0	68.9	86.4	H(26)-C(24)-N-C(31)	158.7
C(9)-C(10)-N-H$^+$	175.8	175.8	180	-30	H(27)-C(24)-N-C(31)	42.2
C(10)-N-C(24)-C(25)	153.8	158.2	-61.5		C(24)-N-C(31)-C(32)	162.4
C(10)-N-C(31)-C(32)	-72.0	-54.6	156.7	68.4	C(32)-C(31)-N-H$^+$	44.9

[a]From ref. 13. [b]From ref. 14. [c]From ref. 15.

crystals, except the values reported[12] for PRC-HCL, which tend to differ substantially from the other values. In the hydrochloride salt the quinonoid character is stronger than in the other crystal structures, whereas it is very low or non-existent in the chlorhydrate of procaine N-D-glucoside monohydrate[16] (PRC-NDG). This is because the protonated tertiary amino nitrogen atom N(23) in the PRC-HCL crystal is hydrogen bonded to a chloride ion which also interacts with two *p*-amino groups[13]. These strong nitrogen-chloride interactions therefore affect not only the conformation of the alkylamino end of the molecule but also increase the quinonoid character of the *p*-aminobenzoate group.

The exocyclic bonds C(1)-C(7) and C(4)-N(12) in PRC-H^+ are shorter than single bonds in most molecules. The C(4)-N(12) distance predicted by AM1 (1.3658 Å) is very close to that reported for the hydrochloride salt[13] (1.359 Å) and for the dihydrogen phosphate salt[8] (PRC-DPH), 1.357 Å. The low quinonoid character predicted by AM1 shows up in the valency angles in the ring, where the two angles at the carbon atoms defining the *para* positions average 118.8° compared with a mean value of 120.6° for the other four endocyclic angles.

The *p*-amino group and the carboxyl group are predicted to be planar by AM1, compared with *tilts* of 2° and 2.5° for PRC-PNP, 28° and 7.5° for PRC-HCl and, 4° and 6.6° for the PRC-DPH salt. In the tertiary amine, the proton $H^+(38)$ is situated with a *tilt* angle out of the C(24)-N-C(31) plane of 57.83°, this plane being tilted with respect to the C(10)-N(23) bond by 48.86°. The orientation of the N(23)-H^+ bond has been shown to be important in the formation of hydrogen bonds with receptors[18].

The major portion of the molecule, extending through atom C(9), is predicted to be planar by AM1. Atom C(10) is coplanar with a C(7)-O(8)-C(9)-C(10) torsional angle of 179.03°, a value that correspond to the *trans* conformation commonly observed in esters.

The conformational flexibility of the procaine molecule has been examined[18] by ^{1}HNMR and quantum chemical calculations[19]. Much attention has been focused on the torsional angle of the OCCN fragment in the side chain. In its conformation this segment resembles a number of other biological compounds containing this moiety[2,18].

The intramolecular distances calculated in the molecule of PRC-H^+, together with the data reported[12-15] for the crystal structure are listed in Table 4. The results for PRC and several other related compounds that contain functional groups similar to the C(24)-N-C(10)-C(9)-O(8) moiety of PRC have been reviewed[20]. The proximity of the ammonium nitrogen atom to the ether oxygen atom (3.17 Å in acetylcholine systems[13]) and the orientation of ammonium substituents relative to the ether oxygen atom have been reported to be important features necessary for effector-receptor interaction.

VIBRATIONAL FREQUENCIES

Solid state

Table 5 shows the observed bands with their estimated intensities, columns eighth-tenth. Non-deuterated in the Table means that the compound was not deuterated; deuterated refers to the deuterated compound.

The frequencies calculated by AM1 are listed in the column second. The relative intensities given in the sixth column are determined by dividing the

Table 4. Comparison of selected intramolecular distances (in Å) in the PRC-H^+ cation with those in the crystal structures of several salts.

Distance	Calculated	X-ray			
	AM1	PRC-HCL[a]	PRC-HCL[b]	PRC-DPH[c]	PRC-PNP[d]
C(2)···O(8)	2.7794		2.761	2.740	2.797
C(2)···C(24)	6.8007		5.951	5.899	
C(2)···C(31)	7.0568		4.225	4.130	4.439
C(6)···O(8)	3.6811		3.643	3.620	3.650
O(8)···N(23)	3.7018	3.07	3.069(4)	3.074(3)	2.983(4)
O(8)···C(24)	4.1969	3.00	3.789	3.823	
O(8)···C(25)	5.6834		5.136	4.799	
O(8)···C(31)	4.3896		2.992	2.952	3.086
O(8)···C(32)	4.9877		3.316	4.435	3.992
O(11)···N(23)	5.0173		4.967(4)	5.022(3)	4.814(5)
C(24)···H^+(38)	2.0651				
C(31)···H^+(38)	2.0594				

[a]From ref. 12. [b]From ref. 13. [c]From ref. 14. [d]From ref. 15.

value of the intensity of each band by the intensity of the strongest (line 86). The characterization of the vibrations is given in the last column. Ring normal modes are numbered according to Wilson's notation[21]. Vibrational mode assignments were made carefully on the basis of group theoretical considerations, published data for disubstituted benzenes[21], isotopic species of the benzoic acid[22], and by comparison with IR and Raman assignments for the benzocaine[3] and procaine[4,5] molecules.

It was necessary to establish a one-to-one correspondence between the frequencies calculated by AM1 and the IR and Raman data. It is not always possible to achieve the desired degree of accuracy in the prediction of a spectrum, because experimental frequencies depend on effects that are not contemplated in the theory, such as solvent shifts, inharmonicity effects, Fermi resonance, etc. To correct this deficiency, sets of scaling factors (or correction factors) have been applied to the computed frequencies and reported for the ab initio[23,24] and semiempirical methods[3,25]. A correction value for each type of vibrational mode was used in this study. The third column lists the available[3,26] scale factors ($\nu_{cal.}/\nu_{exp.}$), and the results obtained appear in the fourth column. The percentage errors in the IR data so determined are presented in the fifth column.

Table 5. Harmonic vibrational frequencies (cm^{-1}) and relative IR intensities for PRC-HCl calculated using the AM1 method and recorded experimentally from IR and Raman spectroscopy in solid and solution phases of PRC-HCL.

No	Theoretical (AM1)						IR	Raman				Characterization
	Frequency	Scale factor used[a]	Scaled frequency	Error (%)[c]	Intensity Relative (%)[a]	Reduced masses	Solid	Solid state		Aqueous solution		
							Non-deuterated	Non-deuterated	Deuterated	Non-deuterated	Deuterated	
1	8				15.2	0						$\tau(NH_2\text{-ring-COO}) + \tau(\text{-}CH_2\text{-}CH_3)$
2	39				13.1	0						$\Gamma(CH_2\text{-N-}(CH_2\text{-}CH_3)_2) + \tau(NH_2\text{-ring-COO})^*$
3	46				15.9	12.3						$\tau(\text{-}CH_2\text{-}CH_2\text{-}) + \tau(NH_2\text{-ring}) + \tau(\text{-}CH_2\text{-}CH_3)$
4	55				18.7	0						$\Gamma(\text{-}CH_2\text{-}CH_3) + \Gamma(NH_2\text{-ring-COO-}CH_2)$
5	71				40.9	0						$\tau(CH19H20) + \tau(COO) + \gamma'(N\text{-ring})$
6	91				27.8	0						$\tau'(N\text{-}CH_2\text{-}CH28H29)$
7	110				35.5	0						$\tau'(\text{-}CH_2\text{-}CH_2\text{-}) + \Gamma(CH_2\text{-}C32H_3) + \gamma(NH_2)^*$
8	114				55.1	4.4						$\gamma(NH_2) + \gamma(C{=}O) + \Gamma(CH29H30)^* + \Gamma(CH35H36)^*$
9	141				39.1	9.1						$\gamma(NH_2) + \tau(C32H_3) + \tau(CH28H30)^*$
10	149				44.0	0						$\gamma(NH_2) + \gamma(COO)^* + \tau(C9H_2)^* + \tau(CH35H37)^*$
11	175				8.0	12.7		155 w	157 w			$\tau(C25H_3) + \tau(CH36H37)^*$
-	-								215 vw			$\gamma(ND_2)$ wagging
12	200				12.1	11.3		231 vw	238 vw			$\tau(C32H_3) + \tau(C31H_2)^* + \tau(CH28H30)^*$
13	245				15.2	5.3		256 sh				$\Gamma(NH_2\text{-ring-COO}) + \Gamma(C31H_2\text{-}CH35H37)$
14	279	1.0388	269	0.7[a]	41.7	0		271 vw	270 vw		266 vw	10b, $\gamma(C\text{-}H) + \gamma(NH_2)$
-	-								280 vw		300 vw	$\tau(ND_2)$ torsion
15	302				19.4	7.8		307 m	307 m	302 s	302 s	$\tau(C10H_2) + \Gamma(COO) + \tau(C32H_3) + \tau(CH29H30)^*$
16	319				15.2	14.3	315 w	328 w	327 w			$\Gamma(C31H_2\text{-}NH^*\text{-}CH_2\text{-}C25H_3)$
17	367	0.9322[b]	394	2.1	6.3	0	402 w?	373 w		404 w		$\tau(NH_2)$ torsion + 16a, $\gamma(CCC)$
-	-								381 vw		368 w	$\gamma(ND_2)$ wagging
-	-							409 w		419 m	422 w	$\gamma(NH_2)$ wagging or $\tau(NH_2)$
18	387				35.7	0	430 w	436 w	437 w			$\Gamma(COO\text{-}CH_2\text{-}CH_2\text{-})$
19	401				13.0	0.4	470 w			460 w	460 vw	$\Gamma(COO\text{-}CH_2\text{-}) + \Gamma^*(NH13) + \Gamma(\text{-}N\text{-}CH_2\text{-})$

(continued)

Table 5. (continued)

-	-								483 w		475 vw	γ(ND_2) wagging
20	430	0.9189[e]	468		8.4	0.3	510 m	510 sh		519 vw		γ(NH_2) wagging
		0.8068[e]	533							602 w		
21	431				18.5	6.1	402 w					τ(NH_2) + γ(C-H) in $C10H_2$, $C24H_2$, $C31H_2$ + γ(C-N) in C31N
22	441	1.0526[e]	419	1.2[g]	26.0	6.4		424 w				Γ(NH_2) + Γ(ring) + Γ(COO-C9)
23	501	0.9899	506	1.8	30.9	0	497 m	500 m	500 m	498 w	493 w	16b, γ(CCC)
24	528				22.5	8.3	570 m			572 w	572 w	Γ($CH_2$9H30-CH27-NH^+-CH33-CH_3)
25	534	1.0526[e]	512		19.1	0.6				559 w	560 w	Γ(NH_2) + Γ(ring-COO-CH_2)
26	647	0.9298	696	0.6	32.8	0	700 s	713 w	714 w	707 w	710 w	4, γ(CCC)
27	660	1.0693[b]	617	1.1	41.0	0	610 m	613 s	613 s	623 vs	621 vs	δ_s(COO) +Γ($C9H_2$-NH^+-C31H_2) +6a, δ(CCC)
28	676	1.0613	637	0.5	23.6	0	640 m	641 s	641 s	641 vs	644 vs	6b, δ(CCC)
29	684				10.8	2.6	655 w	677 sh			658 w	γ(C-H) in $C31H_2$ + δ_s(C10CO) + γ(N-H^+)* + Γ(-CH_2-CH_2-)*
30	747				48.9	0	773 vs	774 w	774 w	778 w	780 w	4 and 5, γ(C-R) and γ(C-H)
31	814				15.1	0.4	740 w			744 m	742 m	γ(C-H) in $C9H_2$, $C10H_2$
32	850				19.8	1.9	800 w			797 m		γ(C-H) in CH_2-CH28H29
33	863				23.0	1.2	818 w					γ(C-H) in CH_2-CH35H36
34	869	1.0429	833		11.1	0.9						10a, γ(C-H)
35	885	1.0178[b]	870	0.2[g]	21.7	0.2		872 s	872 s	859 vs	863 vs	Γ(C-H) in CH_2-CH35H36 + 12, δ(CCC)
36	890	1.0595	840	1.3	41.9	0.8	850 vs	851 vs	851 vs	834 vs		17b, γ(C-H)
37	943				16.2	3.0	902 m	905 sh		908 sh	910 sh	γ(C-H) in CH28H30, CH35H37
38	983	1.0270	957		19.4	0.9						17a, γ(C-H)
39	991	1.0543	940	3.0	25.1	0.8	913 m	918 m	915 m			5, γ(C-H)
40	1003	1.0447[e]	960		8.8	2.6						δ(C-H) in $C10H_2$, CH29H30, CH37
41	1031	1.0057[e]	1025	0.7	24.5	0	1018 m	1025 vw		1020 w	1022 w	δ_{as}(COO) + Γ" (NH_2) + 1, δ(CCC)?
42	1081	1.0447[e]	1035	1.0[g]	31.1	1.2		1046 w	1046 w			δ(C-H) in $C9H_2$, $C10H_2$ + δ(C-H)" in CH27, CH28H30, CH33, CH35H37
43	1100	1.0447[e]	1053	0.3	19.2	1.5	1050 m	1055 w				δ(C-H) in CH20,CH21,$C24H_2$, CH28H29,$C31H_2$
44	1114	1.0526[e]	1058	1.6	12.5	0.6	1075 w	1077 w	1077 w	1089 vw	1073 vw	Γ(NH_2) + δ(C-H) 18a coupled with 19a + δ(C-H)" in CH26, CH29, CH37

45	1117	1.0526[a]	1061	2.0	12.4	1.4	1083 vw					$\Gamma(NH_2)$ + δ(C-H)* in CH26, CH29, CH34, CH36H37
46	1120	1.1110	1008	1.0	18.2	0.9	1018 m	1025 vw		1020w	1022 w	18a, δ(C-H) + δ(C-H) in CH26, CH34, CH36H37
47	1143				19.0	1.6	1118 vs	1118 vw	1118 vw			δ(N-H) in NH38 + δ(C-H) in $C9H_2$, $C10H_2$, $C25H_3$, $C31H_2$, CH35H36
48	1154	1.0447[a]	1105		15.1	0.9						δ(C-H) in $C10H_2$ + δ(C-H)* in $C9H_2$
49	1183	1.0447[a]	1132		12.6	2.1						δ(C-H) in $C24H_2$, CH28H29
-	-										1162 vs	$\beta_s(ND_2)$
50	1191	1.0447[a]	1140	0.3[g]	16.1	1.4		1143 sh		1143 m	1136 m	δ(C-H) in $C31H_2$, CH35H36
51-	1212	1.0133	1196		21.2	1.2						18b, δ(C-H) + δ(C-H) in $C10H_2$, $C24H_2$ + $\Gamma(NH_2)$*
53	1230	1.0447[a]	1177		14.6	3.4						δ(C-H) in CH34 + δ(C-H)* in $C9H_2$, $C24H_2$, CH29, CH36 + δ(N-H)* in NH38
54	1233	1.0447[a]	1180		19.2	3.4						δ(C-H) in $C24H_2$, $C31H_2$ + ν(C-C) in C24C25, C31C32 + δ(C-H)* in $C9H_2$
55	1252	1.0447[a]	1198		15.9	1.2						δ(C-H) in $C9H_2$
56	1255	1.0691	1174	0.1	26.3	0.4	1175 vs	1174 vs	1174 vs	1182 s	1182 s	9a, δ(C-H)
57	1276	1.0039[a]	1271	0.5	38.3	0.5	1278 vs	1267 vs	1267 vs	1281 vs	1278 vs	ν_s(COC) + ν_s(CCO) in C1C7O + 18a, δ(C-H)
58	1295	1.0447[a]	1240	0	23.7	3.1	1240 w	1247 vw	1247 vw			δ_s(C-H) in $C10H_2$, CH27, CH33 + δ(N-H) in NH38
59	1301				30.1	3.1						δ(N-H) in NH38 + δ(C-N) in C24NC31 + δ_s(C-H) in $C10H_2$, CH27
60	1336	0.9844[b]	1357		34.9	0.7						3, δ(C-H)
61	1347	1.0114[a]	1332	1.7	47.2	1.0	1310 s	1311 m	1311 m	1320 s	1323 s	δ_s(C-H) in $C10H_2$, $C24H_2$ and CH33 + ν_{as}(CCO) + δ(N-H) in NH38
62	1353	1.0447[a]	1295		38.4	0.8						δ_s(C-H) in $C10H_2$, $C24H_2$ + δ(N-H)* in NH38
63	1367	1.0447[a]	1309	0.7	30.2	0.7	1318 s					δ_s(C-H) in $C10H_2$, $C31H_2$ + δ_s(C-H)* in $C9H_2$, CH36H37
64	1373	1.0447[a]	1314		23.1	0.9						δ_s(C-H) in $C24H_2$, $C25H_3$, $C31H_2$ + δ_s(C-H)* in CH19, CH21, $C32H_3$

(continued)

Table 5. (continued)

65-	1376	1.0080[e]	1365	0	22.9	1.1	1365 m	1367 m	1367 m	1370 s	1379 w	δ(C-H) in CH_3, $C24H_2$, $C31H_2$ + δ(C-H)* in $C10H_2$
68-	1382	1.0080[e]	1371	0.9	21.5	1.0	1384 m	1380 vw				δ_s(C-H) in CH_3 + δ(C-H)* in $C24H_2$, $C31H_2$
70	1387	1.0447[e]	1328	1.1	23.5	0.7	1343 w					δ_s(C-H) in $C9H_2$ + δ(C-H)* in $C24H_2$, CH36H37
71	1392	1.0136[e]	1373		24.9	1.3						δ_{as}(C-H) in CH_2 + δ(N-H)* in NH38
72	1396	1.0136[e]	1377		23.6	1.3						δ_{as}(C-H) in CH_2 + δ_s(N-H)* in NH38
73	1403	1.0136[e]	1384	1.1	58.1	0.6	1400 s	1392 vw		1393 w	1399 w	δ_{as}(C-H) in $C9H_2$ + 18a, δ(C-H)*
74-	1431	0.9910[e]	1444	0.1	19.3	1.3	1443 s	1449 vw		1449 m	1465 m	δ_{as}(C-H) in CH_3
76	1442	1.0136[e]	1423	0.7	50.4	0.6	1433 s				1444 vw	δ_{as}(C-H) in $C9H_2$
77	1462	1.0451[b]	1399		42.2	0.3						14, ν(C=C) + Γ(NH_2) + δ_{as}(C-H)* in $C9H_2$
78	1470				30.0	2.3	1453 s	1459 vw				δ_s(N-H) in NH38
79	1484				28.3	2.2	1462 s	1466 vw				δ_{as}(N-H) in NH38
80	1575	1.0654[b]	1478	0.1	79.6	0.6	1477 s	1482 vw				19b, ν(C=C) coupled with 18b + ν_{as}(CCO) + δ(NH_2)
81	1589	1.0539	1508	0.8	52.9	0.1	1520 m	1525 m	1525 m	1525 s	1535 m	19a, ν(C=C) coupled with 18a + δ(NH_2)*
82	1689	1.0375[e]	1628		16.7	0.4						δ(NH_2)
83	1727	1.1088	1558	0.9	51.4	0.1	1572 m	1579 m	1580 m	1576 s	1576 m	8b, ν(C=C)
84	1742	1.0618	1641	0.1	93.4	2.5	1640 s	1648 m				β_s(NH_2) + ν(C-N) in CN12 + 19a, ν(C=C)*
85	1770	1.1125	1591	1.1	88.0	0.2	1608 vs	1612 vs	1612 vs	1608 vs	1606 vs	8a, ν(C=C) + β_s(NH_2)*
86	2071	1.2214[e]	1696	0.2	100.0	0	1693 vs	1699 vs	1700 vs	1696 vs	1692 vs	ν(C=O)
-	-										2424 m 2436 m 2448.5 m	ν_s(N-D)
-	-										2466 w 2494 w	ν(N-D) in NHD
-	-								2446 w?		2509.5 w 2528.5 w 2545.5 w	ν_{as}(N-D)

							2720 m?			2680 vw	2680 vw	
87	2964	1.0585[e]	2800	1.1	23.9	0.7	2770 w?	2768 w?		2787 vw		ν_s(C-H) in $C24H_2$ + ν_s(C-H)* in $C10H_2$, $C31H_2$
88-	2967	1.0585[e]	2804	0	32.4	0.7						ν_s(C-H) in $C31H_2$, $C24H_2$, $C10H_2$
90-	3028	1.0486[e]	2888		21.3	0.6						ν_{as}(C-H) in $C24H_2$, $C31H_2$ + ν(C-H)* in CH30, CH35H37
92	3031	1.0486[e]	2890	0.3	25.3	0.6	2880 w	2889 m	2889 m	2909 vw	2896 vw	ν_{as}(C-H) in $C10H_2$ + ν(C-H)* in $C9H_2$
93	3034	1.0585[e]	2866		26.1	0.7						ν_s(C-H) in $C9H_2$ + ν_{as}(C-H)* in $C10H_2$
94-	3045	1.0449[e]	2915	1.0	33.3	0.7		2946 w	2948 w			ν_{as}(C-H) in CH_3 + ν_{as}(C-H)* in $C24H_2$, $C31H_2$
96-	3062	1.0312[e]	2969	0.4	25.2	0.7	2980 w	2982 vs	2981 vs			ν_{as}(C-H) in CH28H29, CH35H36
								2988 vs	2992 vs	2993 vs	2990 vs	
98-	3094	1.0486[e]	2950	0	20.5	0.6	2950 m	2956 m	2961 m	2965 vs	2957 vs	ν_{as}(C-H) in $C9H_2$
100	3149	1.0903[e]	2888		25.7	0.6						ν_s(C-H) in CH_3 mainly on $C25H_3$
101	3150	1.0903[e]	2889	1.0	21.5	0.6	2918 m	2907 sh				ν_s(C-H) in CH_3 mainly on $C32H_3$
102	3162	1.0429[b]	3032	0.6	31.6	0.7		3015 m	3018 vw			7b, ν(C-H) mainly on CH18
103	3176	1.0427[b]	3046	0.2	27.2	0.7	3040 vw	3055 m	3058 m			20a, ν(C-H) mainly on CH16
104	3186	1.0442	3051	0.6	37.0	0.7	3070 vw	3074 s	3077 s	3083 s	3080 m	20b, ν(C-H)
105	3192	1.0433[b]	3060		25.9	0.7						2, ν(C-H)
106	3202				42.7	0.7	2720 m					ν(N-H) in NH38
							2770 w	2768 w				
							3250 sh					
-	-							3211 s	3216 m	3238 s		ν(N-H···)$_{inter.}$ or Fermi resonance
										3251 s		
										3422 sh		
107	3525	1.0196	3457	0.2[f]	41.2	0.8	3350 vs	3351 w		3450 sh	3445 sh	ν_{as}(N-H) in NH_2
										3465 sh		
108	3537	1.0510	3365	0.1[f]	53.2	0.6	3310 vs	3315 m	3309 m	3363 vs	3368 w	ν_s(N-H) in NH_2
										3373 vs		

Abbreviations: vs, very strong; s, strong; m, medium; w, weak; vw, very weak; sh, shoulder; inter, intermolecular; *, very weak contribution of this mode; τ', Γ', nomenclature used according to ref. 3. [a]Calculated $\nu_{AM1}/\nu_{exp.}$ from *p*-aminobenzoic acid. [b]Calculated $\nu_{AM1}/\nu_{exp.}$ from benzene molecule[26]. [c]$100\cdot|\nu_{exp.}-\nu_{AM1\ scaled}|/\nu_{exp.}$ $\nu_{exp.}$ is the IR band in the solid state. [d]Relative to line 86. [e]Calculated $\nu_{AM1}/\nu_{exp.}$ from benzocaine molecule[3]. [f]With Raman frequency in solution phase. [g]With Raman frequency in the solid state.

To facilitate the study of the spectrum, it has been divided in several regions. Fig. 2a shows the non-deuterated compound in the 3500-2800 cm^{-1} range. The antisymmetric and symmetric stretching N-H bands of the *p*-amino group were assigned to the bands at 3351 and 3315 cm^{-1}, respectively. The band at 3211 cm^{-1} was attributed to intermolecular N-H hydrogen bonds. These values and the relation[27]

$$\nu_s(N\text{-}H) = 1023 + 0.682\ \nu_{as}(N\text{-}H) \qquad [1]$$

yielded $\nu_s^{cal} = 3308\ cm^{-1}$, consistent with the value in the Raman spectrum. The values of the force constant of the N-H bond: $K_{NH} = 6.17 \cdot 10^5$ Dyne·cm^{-1} and the angle HNH = 99.32° were obtained using the Linnett equations[28] and were similar to those determined by infrared spectroscopy[5], which confirmed these assignments. In Raman (unlike infrared), the intensity of the band corresponding to the ν_s(N-H) mode was almost double that the ν_{as}(N-H) mode whose intensity was weak, and also double that of the $\nu(N\text{-}H\cdots)_{inter.}$ mode.

In the deuterated sample, Fig. 2b, the decrease in intensity was higher in the bands for ν_{as}(N-H) and $\nu(N\text{-}H\cdots)_{inter.}$ than for ν_s(N-H), which remained nearly unchanged. This led to a weak intensity in the ν_s(N-D) band, which makes it difficult to determine in the spectrum, and a clear band centered at 2446 cm^{-1} and tentatively assigned to ν_{as}(N-D). Unlike the case of PRC[29], the stretching bands corresponding to the ν(NHD) groups were not observed in the Raman and infrared spectra of PRC-HCL.

The 1900-700 cm^{-1} range, in Fig. 3a, showed an increase in the frequency of the ν(C=O) mode appearing at 1693 cm^{-1} (IR) and 1699 cm^{-1} (Raman) compared to that of PRC[4], 1665 cm^{-1} (IR) and 1671.5 cm^{-1} (Raman), which is consistent with a decrease in ν(C-N). This was caused by a slight decrease in the quinonoid character of the ring on formation of the chlorhydrate. Depolarization of the $\Gamma(NH_2)$ mode and the appearance of weak intensity in several ring modes were also observed in this range.

In the deuterated molecule, Fig. 3b, neither the scissor modes $\beta_s(NH_2)$ and $\beta_s(ND_2)$ nor bending modes in the NHD groups were identifiable.

The torsion and wagging modes of the *p*-amino group appear in the 700-100 cm^{-1} range, Fig. 4. Thus, the shoulder at 510 cm^{-1} disappeared on deuteration of the sample; in contrast there was a weak band at 381 cm^{-1}, which on the basis of its shape and position in the spectra was assigned to the $\gamma(NH_2)$ and $\gamma(ND_2)$ wagging modes, respectively. The bands at 483, 409, and 215 cm^{-1}, were also related to this mode, associated with transitions between inversion energy levels.

The bands at 373 cm^{-1} and 280 cm^{-1} have been assigned to the $\tau(NH_2)$ and $\tau(ND_2)$ torsional modes, respectively. The $\tau(NH_2)/\tau(ND_2)$ ratio was in accordance with theoretical calculations[30]. The bands corresponding to the NHD groups have not been identified.

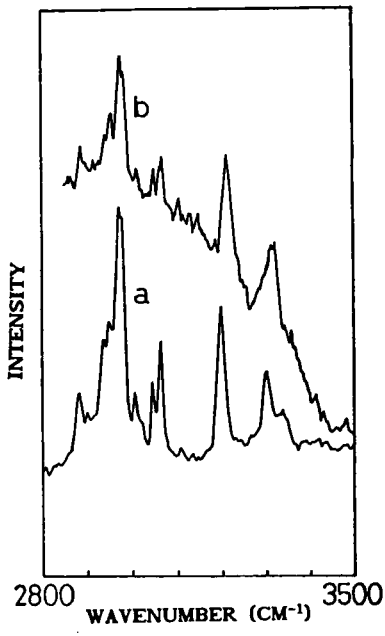

Fig. 2. Raman spectra of PRC-HCL in the solid state. a) Non-deuterated. b) Deuterated.

Aqueous solution

Figs. 5-8 depict the spectra, and Table 5, the eleventh-twelve columns, list the bands observed in the spectra. Band assignments are given in the last column.

Fig. 5a shows the spectrum for the non-deuterated sample in the 3700-2600 cm^{-1} range. Comparing the spectrum with Fig. 2a, there was: a general increase in the frequencies of the bands in accordance with the break of the crystal structure and thus the greater freedom of the molecules in solution than in the solid state. In the amino group, this increase was very high, ca. 100 cm^{-1} for ν_{as}(N-H) and ca. 50 cm^{-1} for ν_{s}(N-H).

A number of bands chiefly related to δ(C-H), several overtones, and combination bands were not identified in the spectrum in aqueous solution.

The splitting of a single band into several bands, was observed in the stretching modes ν_{as}(N-H) (weak bands at 3465, 3450, and 3422 cm^{-1}) and ν_{s}(N-H) (strong bands at 3373 and 3363 cm^{-1}).

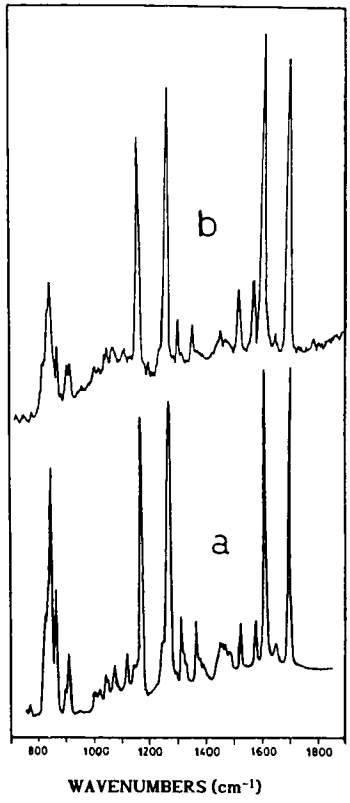

Fig. 3. Solid state, a) non-deuterated, b) deuterated.

The N-H stretching bands satisfy the relation [1]; thus, for the average value (3446 cm^{-1}) of the frequency of the ν_{as}(N-H) mode, is obtained a ν^{s}_{cal} = 3373 cm^{-1}, which differs from the experimental average value by an amount within the standard deviation values for the equation.

The mean values of the frequencies ν_{as}(N-H) and ν_{s}(N-H) were used to calculate the force constant K_{NH} and the HNH angle of the amino group[28] (Table 6). The value of K_{NH} was higher in the solid state (because of the influence of the crystalline field) than in solution. The value of the angle HNH increased in solution due to the low influence of the CL^{-} ion on the hydrogens of the *p*-amino group, because of the greater freedom of these atoms and consequently widening of the angle HNH between both hydrogens. This value

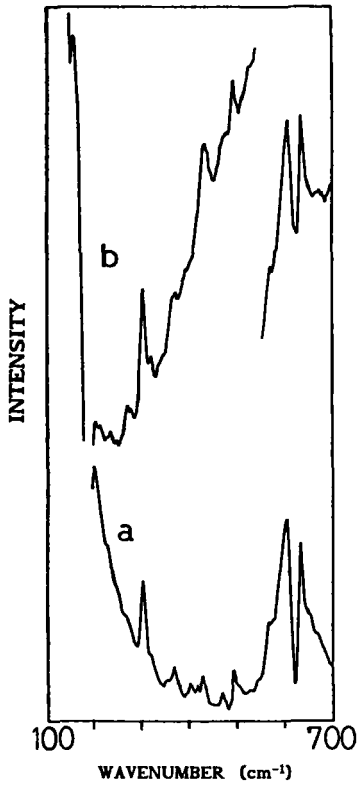

Fig. 4. Solid state, a) non-deuterated, b) deuterated.

was similar to those obtained for benzocaine and procaine of free basis[4,5], without the influence of the CL^- ion of the chlorhydrate.

In the deuterated molecule, the spectral range between 2200 and 3700 cm^{-1} is plotted in Figs 5b and 6. No band is clearly visible in Fig. 6a, because of interference by the spectrum[31] of D_2O. Fig. 6c represents the result of removing this interference by subtracting a previous record of the spectrum of D_2O (Fig. 6b) from the spectrum of the sample using a computer program installed in the Laser-Raman spectrophotometer. This Figure 6c shows clearly identifiable the bands related to the ν(N-D) modes (Table 5). The bands at 2545.5, 2528.5 and 2509.5 cm^{-1} were assigned to ν_{as}(N-D), while the higher intensity bands at 2448.5, 2436 and 2424 cm^{-1} were assigned to the symmetric

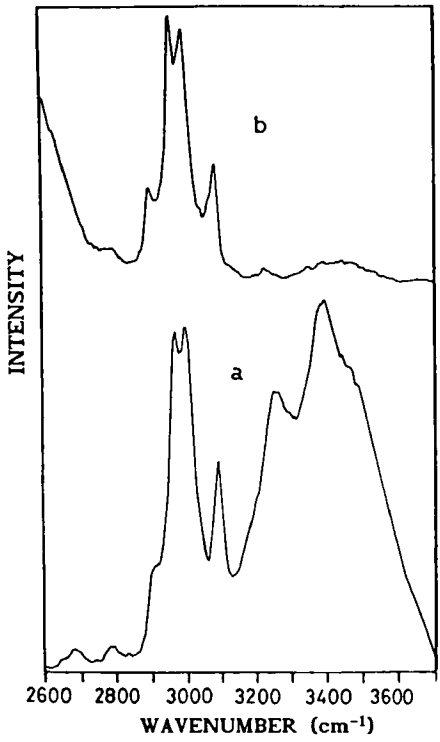

Fig. 5. PRC-HCL in aqueous solution, a) non-deuterated, b) deuterated.

mode. The mean values of the relations $\nu_{as}(N\text{-}H)/\nu_{as}(N\text{-}D) = 1.363$ and $\nu_{s}(N\text{-}H)/\nu_{s}(N\text{-}D) = 1.382$ were in consonance with the data for the solid state and with those for other local anesthetics[4,5]. Using these bands in the equation

$$\nu_{s}(N\text{-}D) = 723.4 + 0.682\ \nu_{as}(N\text{-}D) \qquad [2]$$

yielded a low deviation of 11.2 cm^{-1}, a little higher than for the non-deuterated compound. The Linnett[28] equations, were used to calculate the values shown in Table 6. There was generally good agreement between the values for the non-deuterated molecule and those for the deuterated form.

In contrast to the results obtained for the solid state, in solution the N-H stretching modes disappear totally in the isotopic change, with two bands appearing at 2494 and 2466 cm^{-1}, which were assigned to the N-D stretching mode in NHD groups.

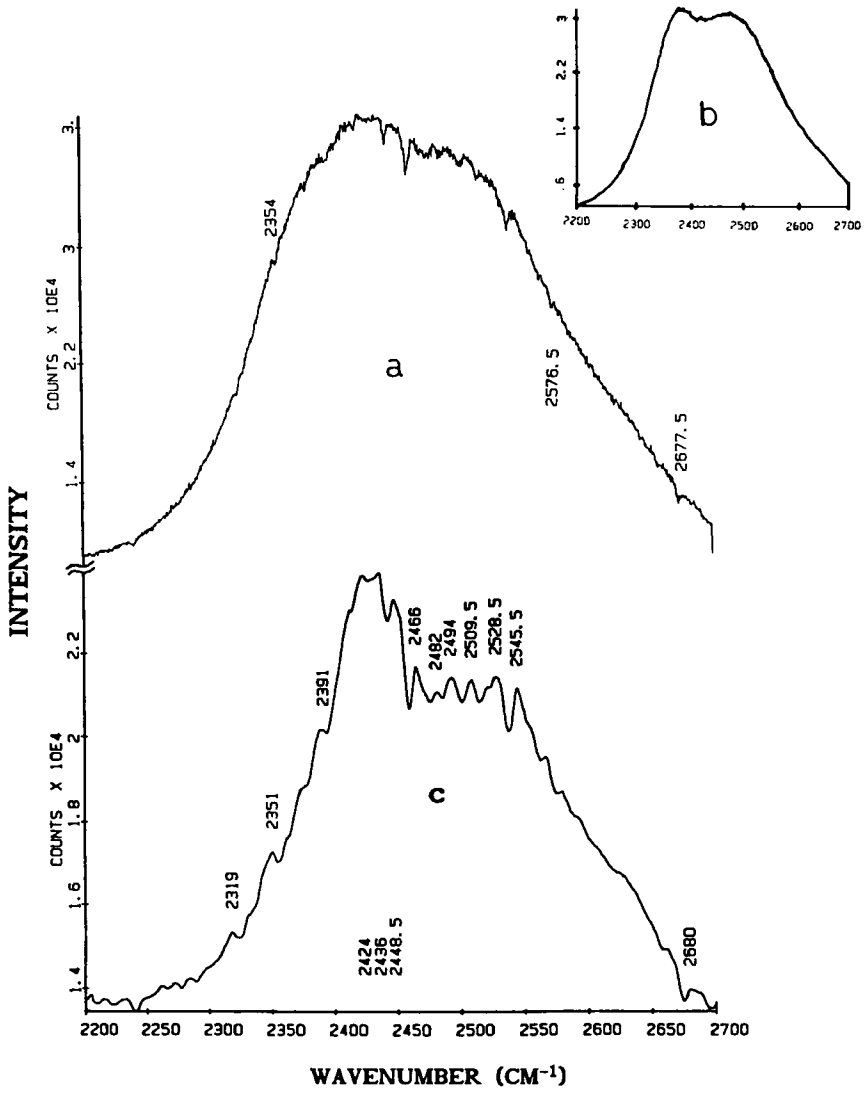

Fig. 6. Raman spectra with laser of 200 mω, 514.5 nm, slits = 300 mic, and points spaced by 0.5 wavenumbers a) solution of PRC-HCL in D_2O, b) D_2O, c) subtraction of b) from a).

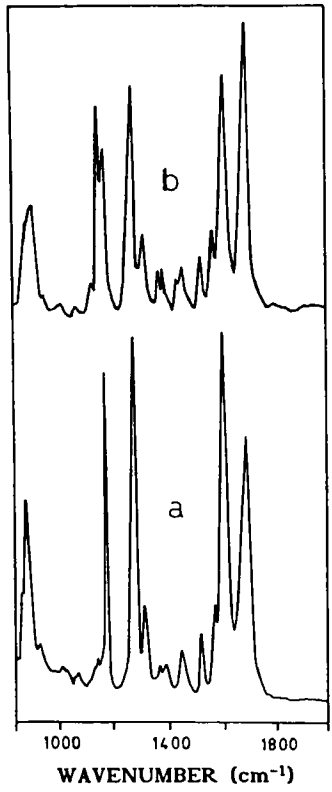

Fig. 7. Aqueous solution of PRC-HCL, a) Non-deuterated, b) deuterated.

Fig. 7a depicts the spectrum of the non-deuterated sample in the 800-2000 cm^{-1} range. In contrast to the solid state, many new bands appeared in the 1700-2000 cm^{-1} range and were assigned to overtones or combination bands. The bands corresponding to the modes $\beta_s(NH_2)$, $\Gamma(NH_2)$ and several δ(C-H) and δ(C-N) in the tertiary amine were not identified. Ring modes 19b and 5 were not observed.

The deuterated form is shown in Fig. 7b. In the spectrum is not identified the high intensity band at 834 cm^{-1} and assigned to the ring mode 17b, γ(C-H).

Fig. 8 depicts the Raman spectrum in the 800-200 cm^{-1} range. Based on their broad form and position in the spectrum, the bands at 602 and 519 cm^{-1}

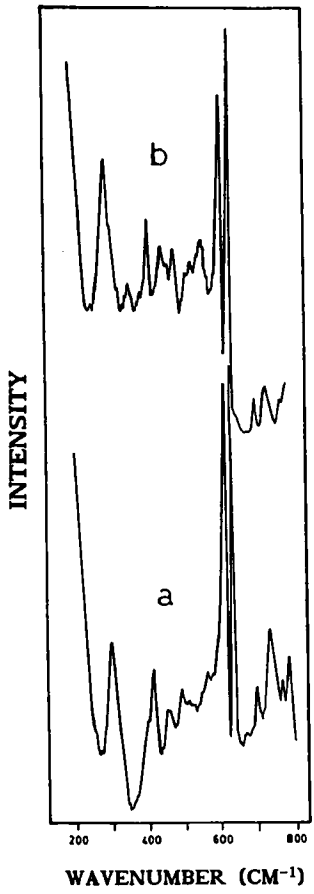

Fig. 8. Aqueous solution of PRC-HCL, a) Non-deuterated, b) deuterated.

were assigned to the wagging mode of the NH_2 group, while those centered at 475 and 368 cm^{-1} corresponding to the $\gamma(ND_2)$, with a non-deuterated/deuterated ratio close to 1.35, in consonance with theoretical calculations[30]. These bands appear at slightly lower frequencies than in the solid state, consistent with the increase in the frequencies for the stretching and torsion modes.

Deuteration of the sample brought about a decrease in the intensity of the bands at 460 and 419 cm^{-1}, associated with amino group modes.

Table 6. Values of the force constant ($K_{NH\ or\ ND}$) in mdynes $Å^{-1}$, and the angle θ between the two N-H bonds in degrees, calculated for the *p*-amino group of PRC-HCL in aqueous solution.

p-amino group	Mean value $\nu_s(cm^{-1})$	Mean value $\nu_{as}(cm^{-1})$	$K_{NH\ or\ ND}$	$\theta_{H\ or\ D}$
$-NH_2$	3368	3445.7	6.45	110.0
$-ND_2$	2436.2	2527.8	6.42	107.2

SUMMARY AND CONCLUSIONS

Except for large differences in several of the torsion angles of the diethyl-amino group, the conformation of the PRC cation was similar for AM1 and the five salts. In all these structures, the cation assumes a *trans* conformation about the O(8)-C(9) bond. For C(9), C(10), and the non-hydrogen atoms in the *p*-aminobenzoate moiety, the rotations by AM1 are small enough to attain an almost planar conformation.

Strong intermolecular hydrogen bonds were observed in the solid state of this compound, through the chlorine atoms of the hydrochloride. On transformation of the procaine molecule to its hydrochloride form, the stretching frequency of the C=O mode increased and the C-N mode decreased, as a result of the differing natures of the intermolecular bonds in PRC and PRC-HCL and the loss of the quinonoid character of the benzene ring.

The good agreement for the frequencies of the antisymmetric and symmetric N-H stretching modes with equation [1] indicates symmetric N-H bonds in the *p*-amino group, with similar electron density. Thus, the bands corresponding to the N-H and N-D modes in amino groups partially deuterated NHD were not observed. In aqueous solution, the slight discrepancy in the values relative to equation [1] originated the N-D stretching bands in NHD groups.

The non-deuterated/deuterated ratios were consistent with the rules of the isotopic change in the spectal frequencies for the *p*-amino group.

The bands for the torsion and wagging modes of the *p*-amino group were detected and identified.

ACKNOWLEDGEMENT

The author wishes to thank the Molecular Spectra Laboratory at the "Daza de Valdes" Optics Institute (CSIC) in Madrid for recording the Raman spectra, and also Mrs M. Santos, L. Lopez and J. Abellanato for their help in the experimental measurements.

REFERENCES

1. J. Büchi, and X. Perlia, in E.J. Arriëns (Ed.), *The Design of Local Anesthetics*, vol. **3**, Academic Press, New York, 1972.

2. J.A. Bevan and J.H. Thompson (Eds.), *Essentials of Pharmacology*, Harper & Row, Publishers, 1983.

3. M. Alcolea Palafox, *J. Mol. Struct. (Theochem.)*, **236**, 161 (1991).

4. M. Alcolea Palafox, *Rev. Roum. Chim.*, **34**, 8, 1667 (1989); *Vibrational Spectrosc.*, **6**, 149 (1 994); *J. Raman Spectrosc.*, **20**, 765 (1989).

5. M. Alcolea Palafox, *Spectrochim. Acta*, **44A**, 12, 1465 (1988).

6. M.J.S. Dewar, E.G. Zoebisch, E.F. Healy and J.J.P. Stewart, *J. Am. Chem. Soc.*, **107**, 3902 (1985).

7. D.A. Liotard, E.F. Healy, J.M. Ruiz and M.J.S. Dewar, in R.D. Dennington, II and E.F. Healy (Eds.), *AMPAC MANUAL. Version 2.1. A General Molecular Orbital Package*, Univ. of Texas at Austin, USA (1989).

8. M.J.S. Dewar and J.J.P. Stewart, *Q.C.P.E. Bull*, **6**, 506 (1986).

9. M.J. Frisch, G.W. Trucks, M. Head-Gordon, P.M.W. Gill, M.W. Wong, J.B. Foresman, B.G. Johnson, H.B. Schlegel, M.A. Robb, E.S. Replogle, R. Gomperts, J.L. Andres, K. Raghavachari, J.S. Binkley, C. Gonzalez, R.L. Martin, D.J. Fox, D.J. Defress, J. Baker, J.J.P. Stewart, and J.A. Pople, *GAUSSIAN 92*, Gaussian Inc., Pittsburgh PA, 1992.

10. D.M. Storch, *DRAW: molecule drawing program*, Dewar group, Univ. of Texas at Austin, USA (1984).

11. N. Müller and A. Falk, *BALL AND STICK Program*, Version 2.2r4, Austria, 1981-89.

12. R. Beall, J. Herdklotz and R.L. Sass, *Biochem. Biophys. Res. Commun.*, **39**, 3, 329 (1970).

13. D.D. Dexter, *Acta Crystallogr.*, Sect. **B**, **28**, 77 (1972).

14. G.R. Freeman and C.E. Bugg, *Acta Crystallogr.*, Sect. **B**, **31**, 96 (1975).

15. M. Sax, J. Pletcher and B. Gustaffson, *Acta Crystallogr.*, Sect. **B**, **26**, 114 (1970).

16. P.O. Dideberg, J. Lamotte and L. Dupont, *Acta Crystallogr.*, Sect. **B**, **36**, 1500 (1980).

17. T.F. Lai and R.E. Marsh, *Acta Crystallogr.*, **22**, 885 (1967).

18. H.G. Mautner, in E. Bergmann and B. Pullman (Eds.), *Molecular and Quantum Pharmacology*, Reidel, Dordrecht, 1974.

19. B. Pullman and Ph. Courriere, *Theor. Chim. Acta*, **31**, 19 (1973).

20. S. Kashino, M. Ikeda and M. Haisa, *Acta Crystallogr.*, **38B**, 1868 (1982).

21. G. Varsanyi, *Assignment for Vibrational Spectra of Seven Hundred Benzene Derivatives*, Vol. 1, Adam Hilger, London, 1974.

22. Y. Kim and K. Machida, *Spectrochim. Acta*, **42A**, 881 (1986).

23. H.F. Hameka, S.L. Emery, G.R. Famini, J.O. Jensen, J.M. Leonard and D.J. Reutter, *Phosphorus Sulfur and Silicon*, **53**, 273 (1990).

24. H.F. Hameka, *J. Mol. Struct. (Theochem.)*, **226**, 241 (1991).

25. M.B. Coolidge, J.F. Marlin and J.J.P. Stewart, *J. Comput. Chem.*, **12**, 948 (1991).

26. M. Alcolea Palafox, *Spectrosc. Letters.*, in preparation.

27. P.J. Krueger, and H.W. Thompson, *Proc. Roy. Soc. (London)*, **243 A**, 143 (1957); and **250 A**, 22 (1959).

28. C.N.R. Rao, *Chemical Applications of Infrared Spectroscopy*, Academic Press, New York, 1963.

29. M. Alcolea Palafox, *Spectrosc. Letters*, **27**, 5, 613 (1994).

30. M. Alcolea Palafox, *Rev. Roum Chim.*, **37**, 5, 541 (1992).

31. G.E. Walrafen, *J. Chem. Phys.*, **48**, 1, 244 (1968).

Date Received: January 13, 1997
Date Accepted: February 25, 1997